INTERNATIONAL JOURNAL FOR NUMERICAL METHODS IN FLUIDS, VOL. 13, 1055–1070 (1991)

THE TWO-DIMENSIONAL TRANSMISSION AND REFLECTION OF A SOLITARY WAVE

Q. Q. LU

Service TV, INRS, Avenue de Bourgogne, F-54501 Vandoeuvre, France

SUMMARY

In the present paper, limited to the discussion of weak non-linear shallow water waves, the transmission and reflection of a planar soliton on a two-dimensional structure are considered. The whole flow field is divided mainly into two subfields. One is in the vicinity of the structure, called the inner field; the other is far from the structure, called the outer field. In the outer field, according to its definition, the influence of the structure on the flow is negligible; to the order $O(\alpha, \beta)$ the governing equation for the flow is replaced by the Boussinesq equation. In the inner field the effect of the structure on the flow is significant, so the full Laplace equation is adopted as the governing equation for the flow field. Then the matched asymptotic expansion method is employed to connect smoothly the inner and outer solutions. Owing to the irregularity of the bottom of the structure, the boundary element method is incorporated. As an example, the case in which the incoming wave is a solitary wave is calculated and the time histories of transmitted and reflected waves are plotted.

KEY WORDS Matched asymptotic expansion Solitary wave Shallow water waves

1. INTRODUCTION

The problem of the diffraction of incident waves by a finite obstacle is of general interest in wave theory. During the past few years, in order to deal with the behaviour of water waves around a structure, linear diffraction theory, the Stokes expansion procedure and direct simulation of the Laplace equation with the full non-linear free surface condition have been developed. It is obvious that the first and second methods are not applicable to the weak non-linear shallow water wave problem to be considered here. With the last kind of method, Isaacson,[1] using a boundary element technique, calculated the interaction between a solitary wave and the structure. However, some problems arise in the direct simulation method (DSM). It is known that the Laplace equation with a full free surface condition admits the solitary wave solution only under some approximations. Owing to the existence of the higher terms in the DSM, the solitary wave suffers significant distortion in its propagation, so the calculated results are the interaction of the solitary wave and the structure with higher-order effects.

The present paper develops further the method the author and his co-workers have established based on the earlier work of Sugimoto and Kakutani.[2] In our method, in the vicinity of the structure the Laplace equation is used as the governing equation; in the region far from the structure the effect of the structure on the flow field can be neglected, so that to the order $O(\alpha, \beta)$ the Boussinesq equations, which admit a solitary wave solution, are adopted as the governing equations. In the overlapping region of the inner and outer fields the matched asymptotic method is used to connect smoothly the solutions of the two fields. By the same procedure the author and

0271–2091/91/181055–16$08.00

Received September 1990
Revised February 1991

his co-workers solved successfully the reflection and transmission of a planar soliton around a rectangular structure[3] and the reflection of a solitary wave on a coastline with a slot.[4]

2. FORMULATION OF THE METHOD

Consider the two-dimensional motion of an inviscid and incompressible fluid bounded by a free surface, a sea bed and the immersed surface of the structure. As shown in Figure 1, a two-dimensional co-ordinate system is employed with its y-axis pointing upwards and its origin 'o' located on the ocean bed. In the present paper the ocean bed is assumed to be flat and the x-axis lies on the sea bed pointing to the right. The two-dimensional structure under consideration has two vertical walls and its bottom is arbitrarily shaped. The geometrical parameters denoted in Figure 1 are non-dimensionalized by using the undisturbed depth and the wavelength as the vertical and horizontal characteristic lengths respectively. Furthermore, the present paper is limited to the discussion of weak non-linear shallow water waves.

2.1. Discussion of the governing equations for different regions

By considering the relative importance of the effect of the structure on the flow field, the whole flow field can be divided into five main subfields, Σ_1, Σ_2, Σ_3, Σ_4 and Σ_5, which are separated by the four dashed lines shown in Figure 1. The outer field, which is far from the structure, consists of Σ_1 and Σ_5, where the effect of the structure on the flow field is negligible, i.e. the existence of the structure does not change the properties of weak non-linear shallow-water waves there. Therefore the non-dimensional Laplace equation, characterized by the relative amplitude α and the relative shallowness β, is adopted as the governing equation of flow motion,[5]

$$\beta\phi_{xx}+\phi_{yy}=0 \qquad (0<y<1+\alpha\eta), \tag{1}$$

together with the boundary conditions

$$\phi_y=0 \qquad (y=0), \tag{2}$$

$$\phi_y-\beta\eta_t-\alpha\beta\phi_x\eta_x=0 \qquad (y=1+\alpha\eta), \tag{3}$$

$$\eta+\phi_t+\frac{\alpha}{2}\phi_x^2+\frac{\alpha}{2\beta}\phi_y^2=0 \qquad (y=1+\alpha\eta), \tag{4}$$

where ϕ is the velocity potential and η is the elevation of the free surface. Here α and β are two

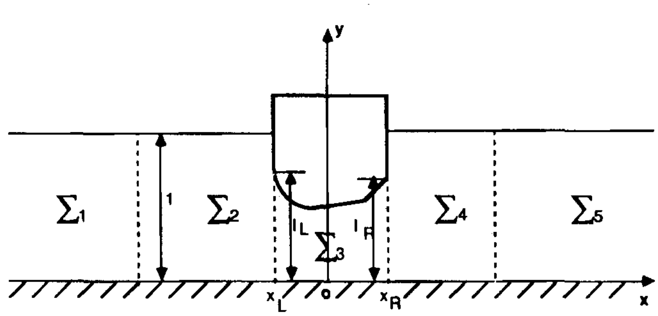

Figure 1. Schematic configuration of the flow field

dimensionless parameters defined respectively by

$$\alpha=\frac{a}{h}, \qquad \beta=\left(\frac{h}{l}\right)^2,$$

where a and l are the typical wave amplitude and length respectively and h is the undisturbed water depth. In the weak non-linear shallow water wave problem $\alpha \approx \beta \ll 1$.

Σ_2, Σ_3 and Σ_4 compose the inner field, where the action of the structure on the waves is significant and, owing to the no-flow condition imposed by the boundary of the structure, the horizontal characteristic length of the flow is also the undisturbed depth h. As a result, in the three subfields equations (1)–(4), non-dimensionalized by taking the wave length l as the horizontal characteristic length, are no longer applicable. Therefore it is obviously necessary that different horizontal scales be used for the inner and outer fields. Let us introduce the co-ordinate transformation

$$\zeta=\frac{x}{\beta^{1/2}}.$$

Here ζ is called the inner variable. Let ζ_{L} and ζ_{R} represent respectively $x_{\mathrm{L}}/\beta^{1/2}$ and $x_{\mathrm{R}}/\beta^{1/2}$. Substituting the inner variable into the Laplace equation (1) and the corresponding boundary conditions, we obtain the dimensionless governing equations for the three inner subfields:

$$\phi_{\zeta\zeta}+\phi_{yy}=0 \qquad (0<y<1+\alpha\eta), \tag{5}$$

$$\phi_y=0 \qquad (y=0), \tag{6}$$

$$\phi_y-\beta\eta_t-\alpha\phi_\zeta\eta_\zeta=0 \qquad (y=1+\alpha\eta), \tag{7}$$

$$\eta+\phi_t+\frac{\alpha}{2\beta}(\phi_\zeta^2+\phi_y^2)=0 \qquad (y=1+\alpha\eta), \tag{8}$$

$$\phi_\zeta=0 \qquad (\zeta=\zeta_{\mathrm{R}}, l_{\mathrm{R}}<y<1+\alpha\eta), \tag{9}$$

$$\phi_\zeta=0 \qquad (\zeta=\zeta_{\mathrm{L}}, l_{\mathrm{L}}<y<1+\alpha\eta), \tag{10}$$

$$\phi_y-\phi_\zeta b'(\zeta)=0 \qquad (y=b(\zeta)), \tag{11}$$

where the function $y=b(\zeta)$ represents the bottom of the structure and the prime denotes its derivative with respect to ζ.

2.2. Solution of the outer field

From equations (1)–(4) we can obtain the formal solution for the outer field $\Sigma_1+\Sigma_5$:

$$\phi(x, y, t)=\sum_{n=0}^{\infty}\left(-\beta y^2\frac{\partial^2}{\partial x^2}\right)^n\frac{f(x,t)}{(2n)!}. \tag{12}$$

In the weak shallow water wave problem equations (1)–(4) can be replaced equivalently to the order $O(\alpha,\beta)$ by the depth-averaged Boussinesq equations

$$\eta_t+[(1+\alpha\eta)u]_x=0, \tag{13}$$

$$u_t+\alpha uu_x+\eta_x-\frac{\beta}{3}u_{xxt}=0, \tag{14}$$

where

$$u=\frac{1}{1+\alpha\eta}\int_0^{1+\alpha\eta}\phi_x\mathrm{d}y$$

and u, η and f satisfy

$$f_x=u+\frac{\beta}{6}u_{xx}+O(\beta^2), \tag{15}$$

$$f_t=-\eta-\frac{\alpha}{2}u^2-\frac{\beta}{2}\eta_{tt}+O(\alpha\beta,\beta^2), \tag{16}$$

$$u=f_x-\frac{\beta}{6}f_{xxx}+O(\beta^2), \tag{17}$$

$$\eta=-f_t-\frac{\alpha}{2}f_x^2+\frac{\beta}{2}f_{ttt}+O(\alpha\beta,\beta^2). \tag{18}$$

The detailed derivation of equations (12)–(18) can be found in Reference 5. In this paper we restrict ourselves to the approximation of $O(\alpha, \beta)$ for the problem shown in Figure 1, so that equations (13) and (14) will be used as the governing equations for the outer field $\Sigma_1+\Sigma_5$.

2.3. Solutions of the inner fields Σ_2 and Σ_4

As explained in Section 2.1, the solution (12) is not applicable for the inner field, i.e. the solution (12) is not uniformly valid in Σ_1 and Σ_2 as well as in Σ_4 and Σ_5. Now we discuss the derivation of the inner solution for the region Σ_2. Introducing a new variable x_1 defined by $x_1+x_L=x$, substituting x_1 into solution (12) with x and x_L being replaced by $\beta^{1/2}\zeta$ and $\beta^{1/2}\zeta_L$ respectively and then expanding $f(\zeta, t)$ in terms of β, we write the first three terms of the resulting expression and denote it by ϕ_∞^-:

$$\phi_\infty^-=f^-+\beta^{1/2}f_x^-(\zeta-\zeta_L)+\frac{\beta}{2}f_{xx}^-[(\zeta-\zeta_L)^2-y^2]+O(\beta^{3/2}). \tag{19}$$

For relation (18) we follow the same procedure and denote the resulting expression by η_∞^-:

$$\eta_\infty^-=-f_t^--\beta^{1/2}f_{xt}^-(\zeta-\zeta_L)-\frac{\alpha}{2}(f_x^-)^2+\frac{\beta}{2}[f_{xxt}^--f_{xxt}^-(\zeta-\zeta_L)^2]+O(\alpha\beta^{1/2},\beta^{3/2}). \tag{20}$$

Similarly, for region Σ_4 we have

$$\phi_\infty^+=f^++\beta^{1/2}f_x^+(\zeta-\zeta_R)+\frac{\beta}{2}f_{xx}^+[(\zeta-\zeta_R)-y^2]+O(\beta^{3/2}), \tag{21}$$

$$\eta_\infty^+=-f_t^+-\beta^{1/2}f_{xt}^+(\zeta-\zeta_R)-\frac{\alpha}{2}(f_x^+)^2+\frac{\beta}{2}[f_{xxt}^+-f_{xxt}^+(\zeta-\zeta_R)^2]+O(\alpha\beta^{1/2},\beta^{3/2}). \tag{22}$$

In later discussion the values associated with f with superscript + or − indicate that they are evaluated at x_R or x_L respectively, and for convenience the variables with subscript 2, 3 or 4 represent the corresponding variables in the region Σ_2, Σ_3 or Σ_4. In fact, according to the matching principle, equations (19)–(22) are the asymptotic expressions of ϕ_2, η_2 and ϕ_4, η_4 as $\zeta\to-\infty$ and ∞ respectively. On the basis of the asymptotic expressions of ϕ_2 and ϕ_4, we construct ϕ_2 and ϕ_4 as follows:

$$\phi_2=\phi_\infty^- +\beta^{1/2}\psi^-(\zeta,y,t), \tag{23}$$

$$\phi_4=\phi_\infty^+ +\beta^{1/2}\psi^+(\zeta,y,t), \tag{24}$$

where ψ^- and ψ^+ are modifying terms for ϕ_∞^- and ϕ_∞^+ due to the effect of the structure. Substituting equations (23) and (24) into equations (5)–(10), we obtain the following governing equations for the functions ψ^- and ψ^+:

$$\psi_{\zeta\zeta}^\pm+\psi_{yy}^\pm=0 \qquad (0<y<1), \tag{25}$$

subject to the boundary conditions

$$\psi_y^\pm=0 \qquad (y=0), \tag{26}$$

$$\psi_y^\pm=O(\beta) \qquad (y=1), \tag{27}$$

$$\eta_4=\eta_\infty^+ -\beta^{1/2}\psi_t^+ -\frac{\alpha}{2}[2f_x^+\psi_\zeta^+ +(\psi_\zeta^+)^2]+O(\beta^{3/2},\alpha\beta^{1/2}) \qquad (y=1), \tag{28a}$$

$$\eta_2=\eta_\infty^- -\beta^{1/2}\psi_t^- -\frac{\alpha}{2}[2f_x^-\psi_\zeta^- +(\psi_\zeta^-)^2]+O(\beta^{3/2},\alpha\beta^{1/2}) \qquad (y=1), \tag{28b}$$

$$\psi^\pm\to 0 \qquad (\zeta\to\pm\infty), \tag{29}$$

$$\psi_\zeta^+=-f_x^+ \qquad (\zeta=\zeta_{\mathrm{R}},\, l_{\mathrm{R}}<y<1), \tag{30}$$

$$\psi_\zeta^-=-f_x^+ \qquad (\zeta=\zeta_{\mathrm{L}},\, l_{\mathrm{L}}<y<1). \tag{31}$$

The approximation of the Boussinesq equations to equations (1)–(4) is of the order $O(\alpha,\beta)$. Therefore we only seek the solutions for ψ^- and ψ^+ to the order $O(\beta^{1/2})$, so that equation (27) means that $\psi^-(\zeta,1,t)$ and $\psi^+(\zeta,1,t)$ are zero. Thus the solutions of equations (25)–(27) together with the matching condition (29) take the form

$$\psi^+=\sum_{n=1}^{\infty} b_n(t)\mathrm{e}^{-n\pi(\zeta-\zeta_{\mathrm{R}})}\cos(n\pi y), \tag{32}$$

$$\psi^-=\sum_{m=1}^{\infty} a_m(t)\mathrm{e}^{m\pi(\zeta-\zeta_{\mathrm{L}})}\cos(m\pi y). \tag{33}$$

2.4. The governing equations for Σ_3

The subfield Σ_3, which is under the structure, differs from the other two inner fields Σ_2 and Σ_4 in the fact that there is no longer a free surface condition but a boundary condition imposed by the rigid structure. Taking into account the better adjustment of the boundary integral equation to the geometrical shape of the boundary, we use the boundary integral equation method for the solution of Σ_3. For the present problem the velocity potential ϕ_3 can be expressed by Green's third identity:

$$\phi_3(P)=\oint_\tau \phi_{3n}(Q)G(P,Q)\,\mathrm{d}\tau-\oint_\tau \phi_3(Q)G_n(P,Q)\,\mathrm{d}\tau \quad (P\in\Sigma_3), \tag{34}$$

where Q is the source point, P is the field point and $G(P, Q)$ is the two-dimensional fundamental solution of the Laplace equation. Here the subscript $\mathbf{n}$ denotes the outward unit vector of the boundary τ of the region Σ_3. To determine the distributions of the velocity potential ϕ_3 and its normal derivative in the subfield Σ_3, let the point P approach the boundary τ from the interior of the subfield Σ_3; we have

$$\tfrac{1}{2}\phi_3(P)=\oint_\tau \phi_{3\mathbf{n}}(Q)G(P,Q)\mathrm{d}\tau-\oint_\tau \phi_3(Q)G_{\mathbf{n}}(P,Q)\mathrm{d}\tau \quad (P\in\tau), \tag{35}$$

which is a Fredholm integral equation of the second kind.[6] The solution to the full problem must satisfy certain continuity conditions over the vertical planes seperating the fluid regions, namely

$$\phi_2=\phi_3, \quad \phi_{2\zeta}=\phi_{3\zeta} \quad (\zeta=\zeta_L, 0<y<l_L), \tag{36}$$

$$\phi_3=\phi_4, \quad \phi_{3\zeta}=\phi_{4\zeta} \quad (\zeta=\zeta_R, 0<y<l_R), \tag{37}$$

which assure the continuity of pressure and velocity on these vertical planes.

2.5. Relations of the solutions in different regions

For Σ_1, Σ_2, Σ_3, Σ_4 and Σ_5 we have so far constructed the solutions valid only within the respective regions. Now we begin to look for the relations of these solutions. Applying the mass conservation equation to the subfield Σ_3 taking into account equations (36) and (37), we obtain

$$\int_0^{l_R} \phi_{4\zeta}|_{\zeta=\zeta_R}\mathrm{d}y=\int_0^{l_L} \phi_{2\zeta}|_{\zeta=\zeta_L}\mathrm{d}y.$$

Substituting expressions (23) and (24) for ϕ_4 and ϕ_2 as well as equations (32) and (33) into the equation above, we obtain

$$f_x^+=f_x^-. \tag{38}$$

Using the Fourier formula for equation (32) with consideration of equations (30) and (36), we have

$$\begin{aligned}
-n\pi b_n&=2\int_0^1 \psi_\zeta^+|_{\zeta=\zeta_R}\cos(n\pi y)\mathrm{d}y\\
&=2\left[\left(\int_0^{l_R}\psi_\zeta^+|_{\zeta=\zeta_R}+\int_{l_R}^1\psi_\zeta^+|_{\zeta=\zeta_R}\right)\cos(n\pi y)\mathrm{d}y\right]\\
&=2\int_0^{l_R}\left(\frac{\phi_{3\zeta}|_{\zeta=\zeta_R}}{\beta^{1/2}}-f_x^+\right)\cos(n\pi y)\mathrm{d}y-2\int_{l_R}^1 f_x^+\cos(n\pi y)\mathrm{d}y\\
&=\frac{2}{\beta^{1/2}}\int_0^{l_R}\phi_{3\zeta}|_{\zeta=\zeta_R}\cos(n\pi y)\mathrm{d}y.
\end{aligned}$$

Hence

$$b_n=-\frac{2}{n\pi\beta^{1/2}}\int_0^{l_R}\phi_{3\zeta}|_{\zeta=\zeta_R}\cos(n\pi y)\mathrm{d}y. \tag{39}$$

Similarly,

$$a_m=\frac{2}{m\pi\beta^{1/2}}\int_0^{l_L}\phi_{3\zeta}|_{\zeta=\zeta_L}\cos(m\pi y)\mathrm{d}y. \tag{40}$$

By using equations (39) and (40) and substituting the expressions for ϕ_2 and ϕ_4 into equations (36) and (37), we obtain

$$\phi_3|_{\zeta=\zeta_R} = f^+ - \frac{\beta}{2} f^+_{xx} y^2 + \sum_{n=1}^{\infty} \left(-\frac{2}{n\pi} \int_0^{l_R} \phi_{3\zeta}|_{\zeta=\zeta_R} \cos(n\pi y)\mathrm{d}y \right) \cos(n\pi y), \tag{41}$$

$$\phi_3|_{\zeta=\zeta_L} = f^- - \frac{\beta}{2} f^-_{xx} y^2 + \sum_{m=1}^{\infty} \left(\frac{2}{m\pi} \int_0^{l_L} \phi_{3\zeta}|_{\zeta=\zeta_L} \cos(m\pi y)\mathrm{d}y \right) \cos(m\pi y). \tag{42}$$

The two last equations give the relations of the velocity potential ϕ_3 and its normal derivative on the boundaries $\zeta=\zeta_R$ and $\zeta=\zeta_L$ of Σ_3.

In the outer field the flow is described by η and u, so we must establish the relations between the equations obtained and η and u. By differentiating equations (35), (41) and (42) with respect to time t and then substituting the relations (15) and (16) into the resulting equations to eliminate the function f and its derivatives, we obtain

$$\tfrac{1}{2}(\phi_3(P))_t = \oint_\tau (\phi_{3t})_n(Q) G(P,Q)\mathrm{d}\tau - \oint_\tau \phi_{3t}(Q) G_n(P,Q)\mathrm{d}\tau \quad (P \in \tau), \tag{43}$$

$$\phi_{3t}|_{\zeta=\zeta_R} = -\eta^+ - \frac{\alpha}{2}(u^+)^2 - \frac{\beta}{2}\eta^+_{tt}(1-y^2) + \sum_{n=1}^{\infty} \left(-\frac{2}{n\pi} \int_0^{l_R} (\phi_{3t})_\zeta|_{\zeta=\zeta_R} \cos(n\pi y)\mathrm{d}y \right) \cos(n\pi y), \tag{44}$$

$$\phi_{3t}|_{\zeta=\zeta_L} = -\eta^- - \frac{\alpha}{2}(u^-)^2 - \frac{\beta}{2}\eta^-_{tt}(1-y^2) + \sum_{m=1}^{\infty} \left(\frac{2}{m\pi} \int_0^{l_L} (\phi_{3t})_\zeta|_{\zeta=\zeta_L} \cos(m\pi y)\mathrm{d}y \right) \cos(m\pi y). \tag{45}$$

From equation (38) we can get

$$u^+ = u^-. \tag{46}$$

By differentiating equations (39) and (40) with respect to time t, we have

$$(b_n)_t = -\frac{2}{n\pi\beta^{1/2}} \int_0^{l_R} (\phi_{3t})_\zeta|_{\zeta=\zeta_R} \cos(n\pi y)\mathrm{d}y, \tag{47}$$

$$(a_m)_t = \frac{2}{m\pi\beta^{1/2}} \int_0^{l_L} (\phi_{3t})_\zeta|_{\zeta=\zeta_L} \cos(m\pi y)\mathrm{d}y. \tag{48}$$

So far the system of governing equations for the present problem is not closed, a fact that can be found in the case of Reference 2, where the structure under consideration was a special case of the present problem. Therefore we need to find an additional equation to close the system. Let us apply the two-dimensional Green formula to the field Σ_3 for the velocity potential ϕ_3:

$$\iint_{\Sigma_3} \nabla\phi_3 \mathrm{d}\tau = \oint_\tau \mathbf{n}\phi_3 \mathrm{d}\tau,$$

where ∇ denotes the two-dimensional gradient operator. The last equation can be rewritten as

$$\int_{\zeta_L}^{\zeta_R} \left(\int_0^{b(\zeta)} \nabla\phi_3 \mathrm{d}y \right) \mathrm{d}\zeta = \oint_\tau \mathbf{n}\phi_3 \mathrm{d}\tau.$$

Taking the scalar product of the above equation with the unit vector $\mathbf{i}$ of the x-axis, we have

$$\int_{\zeta_L}^{\zeta_R} \left(\int_0^{b(\zeta)} \mathbf{i}\cdot\nabla\phi_3 \mathrm{d}y \right) \mathrm{d}\zeta = \oint_\tau \mathbf{n}\cdot\mathbf{i}\,\phi_3 \mathrm{d}\tau. \tag{49}$$

Conservation of mass leads to

$$\int_0^{b(\zeta)} \nabla\phi_3\cdot\mathbf{i}\,\mathrm{d}y=\int_0^{l_R}\phi_{4\zeta}|_{\zeta=\zeta_R}\,\mathrm{d}y,$$

which implies that the integral in parentheses in equation (49) is independent of the variable ζ. By substituting the above equation and the expression for ϕ_4 into equation (49) and then differentiating the resulting equation with respect to time t, we obtain the desired additional equation

$$\begin{aligned}\beta^{1/2}(\zeta_R-\zeta_L)u_t^+ = &-\int_{\zeta_L}^{\zeta_R} b'(\zeta)\phi_{3t}\mathrm{d}\zeta+\left(-\eta^+-\frac{\alpha}{2}(u^+)^2\right)l_R-\frac{\beta}{2}\eta_{tt}^+\left(l_R-\frac{l_R^3}{3}\right)\\&+\left(\eta^-+\frac{\alpha}{2}(u^-)^2\right)l_L+\frac{\beta}{2}\eta_{tt}^-\left(l_L-\frac{l_L^3}{3}\right)\\&-2\sum_{n=1}^{\infty}\frac{1}{(n\pi)^2}\left(\int_0^{l_R}(\phi_{3t})_\zeta|_{\zeta=\zeta_R}\cos(n\pi y)\right)\sin(n\pi l_R)\\&-2\sum_{m=1}^{\infty}\frac{1}{(m\pi)^2}\left(\int_0^{l_L}(\phi_{3t})_\zeta|_{\zeta=\zeta_L}\cos(m\pi y)\right)\sin(m\pi l_L).\end{aligned}\tag{50}$$

When the bottom of the structure is flat, equation (50) reduces to equations (28c) and (28d) in Reference 2. Now equations (43)–(46), (50) and the Boussinesq equations (13) and (14) constitute the set of governing equations for the present problem.

3. DISCRETIZATION OF EQUATIONS

Although the present problem has been simplified greatly, it is still quite difficult to obtain the analytical solution, so that additional approximation must be introduced. The discretized forms of the present equations are

$$\sum_{j=1}^{n_t}(\phi_{3t})_j H_{ij}=\sum_{j=1}^{n_t}[(\phi_{3t})_{\mathbf{n}}]_j G_{ij}\quad (i=1,2,3,\ldots,n_t),\tag{51}$$

$$(u^+)^{s+1}=(u^-)^{s+1},\tag{52}$$

$$\begin{aligned}\phi_{3t}|_{\zeta=\zeta_R}=&-(\eta^+)^{s+1}-\frac{\alpha}{2}[(u^+)^{s+1}]^2-\frac{\beta}{2}\frac{(\eta^+)^{s+1}-2(\eta^+)^s+(\eta^+)^{s-1}}{\Delta t^2}(1-y^2)\\&+\sum_{n=1}^{k}\left(-\frac{2}{n\pi}I_n\cos(n\pi y)\right),\end{aligned}\tag{53}$$

$$\begin{aligned}\phi_{3t}|_{\zeta=\zeta_L}=&-(\eta^-)^{s+1}-\frac{\alpha}{2}[(u^-)^{s+1}]^2-\frac{\beta}{2}\frac{(\eta^-)^{s+1}-2(\eta^-)^s+(\eta^-)^{s-1}}{\Delta t^2}(1-y^2)\\&+\sum_{m=1}^{k}\left(\frac{2}{m\pi}I_m\cos(m\pi y)\right),\end{aligned}\tag{54}$$

$$\begin{aligned}(u^+)^{s+1}=(u^+)^s+\frac{\Delta t}{\beta^{1/2}(\zeta_R-\zeta_L)}\Bigg[&I_1-\left((\eta^+)^{s+1}+\frac{\alpha}{2}(u^+)^{s+1}(u^+)^{s+1}\right)l_R\\&+\left((\eta^-)^{s+1}+\frac{\alpha}{2}(u^-)^{s+1}(u^-)^{s+1}\right)l_L-\frac{\beta}{2}\frac{(\eta^+)^{s+1}-2(\eta^+)^s+(\eta^+)^{s-1}}{\Delta t^2}\left(l_R-\frac{l_R^3}{3}\right)\end{aligned}$$

$$-2\sum_{n=1}^{k}\frac{1}{(n\pi)^2}I_n\sin(n\pi l_{\mathrm{R}})-\frac{\beta}{2}\frac{(\eta^-)^{s+1}-2(\eta^-)^s+(\eta^-)^{s-1}}{\Delta t^2}$$
$$\times\left(l_{\mathrm{L}}-\frac{l_{\mathrm{L}}^3}{3}\right)-2\sum_{m=1}^{k}\frac{1}{(m\pi)^2}I_m\sin(m\pi l_{\mathrm{L}})\Bigg], \tag{55}$$

where superscripts $s+1$, s and $s-1$ represent the corresponding time steps. The infinite series in equations (44), (45) and (50) are truncated at the kth term. Equation (51) is the discretized form of equation (43) by using n_t line segments, i.e. boundary elements, to approximate the four boundaries of Σ_3 and letting ϕ_{3t} and $(\phi_{3t})_n$ be constant over each boundary element. The values for ϕ_{3t} and $(\phi_{3t})_n$ over the jth boundary element are denoted respectively by $(\phi_{3t})_j$ and $((\phi_{3t})_n)_j \cdot H_{ij}$ and G_{ij} are known coefficients and their expressions and computation programmes can be found in Reference 7. n_t, made up of n_{R}, n_s, n_{L} and n_b over the four boundaries $\zeta=\zeta_{\mathrm{R}}$, $y=b(\zeta)$, $\zeta=\zeta_{\mathrm{L}}$ and $y=0$ shown in Figure 2, is the total number of boundary elements used. In the present paper the discretization for the four boundaries is respectively uniform.

I_1, I_n and I_m in equations (53)–(55) are the numerical treatments for the integrals

$$\int_{\zeta_{\mathrm{L}}}^{\zeta_{\mathrm{R}}} b'(\zeta)\phi_{3t}\,\mathrm{d}\zeta, \qquad \int_0^{l_{\mathrm{R}}}(\phi_{3t})_\zeta|_{\zeta=\zeta_{\mathrm{R}}}\cos(n\pi y)\,\mathrm{d}y, \qquad \int_0^{l_{\mathrm{L}}}(\phi_{3t})_\zeta|_{\zeta=\zeta_{\mathrm{L}}}\cos(m\pi y)\,\mathrm{d}y$$

and take respectively the following forms:

$$I_1=\sum_{j=n_{\mathrm{R}}+1}^{n_{\mathrm{R}}+n_s}(\phi_{3t})_j\int_{\zeta_j}^{\zeta_{j+1}}b'(\zeta)\,\mathrm{d}\zeta=\sum_{j=n_{\mathrm{R}}+1}^{n_{\mathrm{R}}+n_s}(\phi_{3t})_j\,(y_{j+1}-y_j),$$

where $y_j=b(\zeta_j)$ and $y_{j+1}=b(\zeta_{j+1})$, and

$$I_n=\sum_{j=1}^{n_{\mathrm{R}}}\frac{[(\phi_{3t})_\zeta]_j|_{\zeta=\zeta_{\mathrm{R}}}}{n\pi}[\sin(n\pi y_{j+1})-\sin(n\pi y_j)],$$

$$I_m=\sum_{j=n_{\mathrm{R}}+n_s+1}^{n_{\mathrm{R}}+n_s+n_{\mathrm{L}}}\frac{[(\phi_{3t})_\zeta]_j|_{\zeta=\zeta_{\mathrm{L}}}}{m\pi}[\sin(m\pi y_{j+1})-\sin(m\pi y_j)],$$

where y_j, ζ_j, y_{j+1} and ζ_{j+1} are the co-ordinates of the extreme points of the jth boundary element. Over $\zeta=\zeta_{\mathrm{R}}$ and $\zeta=\zeta_{\mathrm{L}}$, $(\phi_{3t})_j$ and $((\phi_{3t})_\zeta)_j$ are all unknown, so that we have to reduce the number of unknowns in equation (51) in order for it to be solvable. We substitute the discretized forms of equations (53) and (54) into equation (51) to eliminate ϕ_{3t} at the boundaries $\zeta=\zeta_{\mathrm{R}}$ and $\zeta=\zeta_{\mathrm{L}}$. For

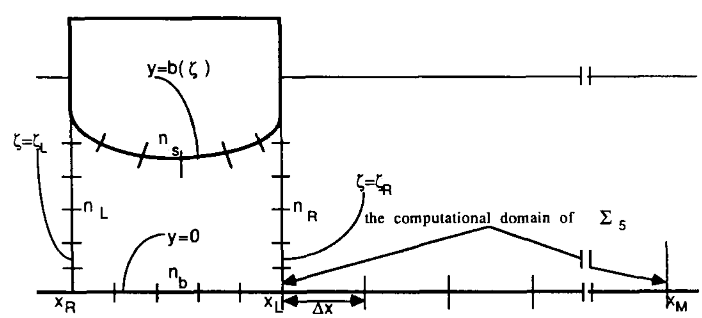

Figure 2. Sketch of the boundaries of Σ_3 and the computational domain of Σ_5 discretized into line segments for equation (51) and the Boussinesq equations

this, y in equations (53) and (54) is replaced by the co-ordinates of the middle points corresponding to the boundary elements. Thus the resulting equation can be expressed in a compact form in terms of unknowns Φ_j, which contain n_t unknown values of $(\phi_{3t})_j$ and $((\phi_{3t})_\zeta)_j$:

$$\sum_{j=0}^{n_t} G^*_{ij}\Phi_j = B_i, \quad i=1,2,\ldots,n_t, \quad \Phi_j = \begin{cases} (\phi_{3t})_j, & j=n_R+1,\ldots,n_R+n_s \text{ or } n_t-n_b+1,\ldots,n_t, \\ ((\phi_{3t})_\zeta)_j|_{\zeta=\zeta_R}, & j=1,2,\ldots,n_R, \\ ((\phi_{3t})_\zeta)_j|_{\zeta=\zeta_L}, & j=n_R+n_s+1,\ldots,n_R+n_s+n_L. \end{cases} \tag{56}$$

Here B_i are functions of variables η^+, u^+, η^- and u^-, and G^*_{ij} are known.

For the Boussinesq equations the following predictor–corrector method is adopted. Here we only describe the treatment of Σ_5, the method for Σ_1 being similar:

$$\eta^*_i = \eta^s_i - \Delta t\,\frac{P^s_{i+1}u^s_{i+1} - P^s_{i-1}u^s_{i-1}}{2\Delta x} + \frac{\alpha(\Delta t)^2}{2\Delta x^2}\,[(u^2P)^s_{i+1} - 2(u^2P)^s_i + (u^2P)^s_{i-1}], \tag{57}$$

$$\frac{u^{s+1}_i - u^s_i}{\Delta t} + \frac{\alpha(u^{s+1}_{i+1}u^s_{i+1} - u^{s+1}_{i-1}u^s_{i-1})}{4\Delta x} + \frac{\eta^*_{i+1} + \eta^s_{i+1} - \eta^*_{i-1} - \eta^s_{i-1}}{4\Delta x}$$

$$- \frac{\beta}{3\Delta t\Delta x^2}(u^{s+1}_{i+1} - 2u^{s+1}_i + u^{s+1}_{i-1} - u^s_{i-1} + 2u^s_i - u^s_{i-1}) = 0, \tag{58}$$

$$\frac{\eta^{s+1}_i - \eta^s_i}{\Delta t} + \frac{1}{4\Delta x}\{[1+0{\cdot}5\alpha(\eta^*_{i+1} + \eta^s_{i+1})](u^s_{i+1} + u^{s+1}_{i+1}) - [1+0{\cdot}5\alpha(\eta^*_{i-1} + \eta^s_{i-1})](u^s_{i-1} + u^{s+1}_{i-1})\} = 0. \tag{59}$$

At the boundary $x = x_R$, where $i=0$, equations (57) and (59) are replaced respectively by

$$\eta^*_0 = \eta^s_0 - \Delta t\left(\frac{P^s_1u^s_1 - P^s_0u^s_0}{\Delta x}\right), \tag{60}$$

$$\frac{\eta^{s+1}_0 - \eta^s_0}{\Delta t} + \frac{1}{2\Delta x}\{[1+0{\cdot}5\alpha(\eta^*_1 + \eta^s_1)](u^s_1 + u^{s+1}_1) - [1+0{\cdot}5\alpha(\eta^*_0 + \eta^s_0)](u^s_0 + u^{s+1}_0)\} = 0, \tag{61}$$

where $P = 1 + \alpha\eta$ and $\eta_0 = \eta^+$. In equation (57), for $i=0$, $u_0 = u^+$. The computational domain is truncated at $x_M = M\Delta x$, as shown in Figure 2, where M is the number of meshes of computation and linear distributions of η and u are assumed at x_M, i.e.

$$\eta^{s+1}_M = 2\eta^{s+1}_{M-1} - \eta^{s+1}_{M-2}, \qquad u^{s+1}_M = 2u^{s+1}_{M-1} - u^{s+1}_{M-2}. \tag{62}$$

The scheme (57)–(62) was tested for relatively extensive initial boundary value problems of the Boussinesq equations. The results show that it has a good performance in predicting the behaviours of the solitary wave.[8,9] Of course, a suitable transparent boundary operator is better for the treatment of the outer boundary x_M, but this is beyond the scope of the present study.

It must be pointed out that the inner and outer solutions are valid only in their respective subfields. Therefore it is necessary to construct complex solutions which are uniformly valid for the inner and outer fields. The complex solutions for the free surface elevation are constructed for $\Sigma_1 + \Sigma_2$ and $\Sigma_4 + \Sigma_5$ respectively as follows:

$$\eta_L = (\eta_B)_L - \beta^{1/2}\psi^-_t - \frac{\alpha}{2}[2f^-_x\,\psi^-_\zeta + (\psi^-_\zeta)^2]$$

$$=(\eta_{\mathrm{B}})_{\mathrm{L}}-\frac{2}{\pi^2}\sum_{j=n_{\mathrm{R}}+n_{\mathrm{s}}+1}^{n_{\mathrm{R}}+n_{\mathrm{s}}+n_{\mathrm{L}}}\Phi_j\sum_{m=1}^{k}\frac{(-1)^m}{m^2}\mathrm{e}^{m\pi(x-x_{\mathrm{L}})/\beta^{1/2}}[\sin(m\pi y_{j+1})-\sin(m\pi y_j)], \tag{63}$$

$$\eta_{\mathrm{R}}=(\eta_{\mathrm{B}})_{\mathrm{R}}-\beta^{1/2}\psi_t^+-\frac{\alpha}{2}[2f_x^+\psi_\zeta^+ +(\psi_\zeta^+)^2]$$

$$=(\eta_{\mathrm{B}})_{\mathrm{R}}+\frac{2}{\pi^2}\sum_{j=1}^{n_{\mathrm{R}}}\Phi_j\sum_{n=1}^{k}\frac{(-1)^n}{n^2}\mathrm{e}^{-n\pi(x-x_{\mathrm{R}})/\beta^{1/2}}[\sin(n\pi y_{j+1})-\sin(n\pi y_j)], \tag{64}$$

where $(\eta_{\mathrm{B}})_{\mathrm{L}}$ and $(\eta_{\mathrm{B}})_{\mathrm{R}}$ are the displacements of the free surface calculated numerically by equations (57)–(62) for Σ_1 and Σ_5 respectively. It can be easily verified that solutions (63) and (64) tend to equations (28a) and (28b) as well as to the solution of the Boussinesq equations as $x \to x_{\mathrm{L}}, x_{\mathrm{R}}, -\infty$ and ∞ respectively.

In the present computation the coefficients a_n and b_m, which are necessitated by equations (63) and (64) through ψ_ζ^- and ψ_ζ^+, are obtained by integrating numerically equations (47) and (48) with respect to time t:

$$a_m=\int_0^{s\Delta t}(a_m)_t\,\mathrm{d}t=\left(\sum_{q=1}^{s-1}(a_m(q\Delta t))_t+0{\cdot}5[(a_m(0))_t+(a_m(s\Delta t))_t]\right)\Delta t, \tag{65}$$

$$b_n=\int_0^{s\Delta t}(b_n)_t\,\mathrm{d}t=\left(\sum_{q=1}^{s-1}(b_n(q\Delta t))_t+0{\cdot}5[(b_n(0))_t+(b_n(s\Delta t))_t]\right)\Delta t. \tag{66}$$

We outline briefly the computational procedure.

1. Give the initial distributions of u and η for the two outer fields Σ_1 and Σ_5.
2. As initial guess value for $(u^+)^{s+1}$ let $(u^+)^{s+1}=(u^+)^s$. Therefore equation (52) leads to $(u^-)^{s+1}=(u^+)^{s+1}$. When $s=0$, to initiate the computation, let $(\eta^+)^{s-1}$ and $(\eta^-)^{s-1}$ be equal to $(\eta^+)^s$ and $(\eta^-)^s$ respectively.
3. Solve respectively the initial boundary value problems of the Boussinesq equations for the two outer fields Σ_1 and Σ_5 by using the scheme (57)–(62) with the values of $(u^+)^{s+1}$ and $(u^-)^{s+1}$ defined in step 1 to obtain $(\eta^+)^{s+1}$ and $(\eta^-)^{s+1}$.
4. Substitute $(u^+)^{s+1}$, $(u^-)^{s+1}$, $(\eta^+)^{s+1}$ and $(\eta^-)^{s+1}$ into the linear equation system (56) so that $(\phi_{3t})_j$ (on the bottom of the structure and the ocean bed), $((\phi_{3t})_\zeta)_j|_{\zeta=\zeta_{\mathrm{R}}}$ and $((\phi_{3t})_\zeta)_j|_{\zeta=\zeta_{\mathrm{L}}}$ can be calculated. By the substitution of these values into equation (55), a new value, which is denoted by $(u^+)^*$, for $(u^+)^{s+1}$ is obtained.
5. Correct $(u^+)^{s+1}$ by $(u^+)^{s+1}=(1-\omega)(u^+)^{s+1}+\omega(u^+)^*$, where ω is the relaxation factor. Then, using the updated $(u^+)^{s+1}$, repeat the loop of execution of steps 1–4 until the difference between $(u^+)^{s+1}$ and $(u^+)^*$ is less than a given error value.
6. Obtain the complex solutions of the elevation of the free surface through equations (63) and (64) with the values calculated from steps 1–5. The computation at the $(s+1)$th time level is completed.

4. EXAMPLES AND DISCUSSION

The method presented in the above sections is established for a general case and can be used to deal with relatively extensive shallow water problems. In the present paper, only the situation where a solitary wave is incident upon the structure from the right-hand side of the field is considered. The initial conditions for η and u are[10]

$$\eta = \operatorname{sech}^2\left(\frac{\sqrt{(3\alpha)}}{2\beta^{1/2}}\right)(x-x_0-x_R), \qquad u = \frac{-(1+\alpha/2)\eta}{1+\alpha\eta} \quad (\text{in } \Sigma_5),$$

$$\eta = 0, \qquad u = 0 \quad (\text{in } \Sigma_1),$$

i.e. the initial position of the incident solitary wave is localized at $x_0 + x_R$. Throughout the present computation, except where noted, the parameters take the following values: $\alpha = 0{\cdot}2$, $\beta = 0{\cdot}1$, $x_0 = 5{\cdot}0$, $k = 20$, $\Delta t = 0{\cdot}03$, $\Delta x = 0{\cdot}08$, $M = 200$, $n_L = n_R = 30$, $n_s = 60$, $n_b = 30$, $\omega = 0.8$.

In the present study, several cases where the structures are symmetrical as shown in Figures 3 and 4 are calculated.

In analogy with other problems that involve time stepping, some conditions must be satisfied by Δt and Δx in order to maintain the stability of the solution. Computations using different values of Δt and Δx show that the whole system of the algorithm remains stable for the values of Δt and Δx satisfying the stability condition of the finite difference scheme (57)–(62), i.e. the whole method has the same stability condition as that of the scheme (57)–(62). In addition, the iteration process in steps 1–5 is convergent for ω between zero and unity, which only affects the speed of convergence. With the optimal value of ω, 0·8, three iterations are used in this paper to obtain a value for $(u^+)^{s+1}$ with a relative error $|(u^+)^{s+1} - (u^+)^*|/(u^+)^*$ of 10^{-4}.

To examine the influences of the structure dimensions and shape on the flow, let us define several characteristic parameters: η^+_{max}, the maximum surface wave elevation at $\zeta = \zeta_R$; t^+_{max}, the

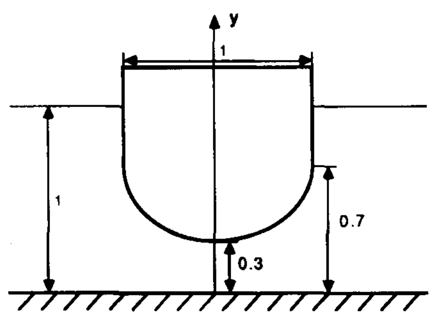

Figure 3. Case 1: the bottom of the structure is part of a circle

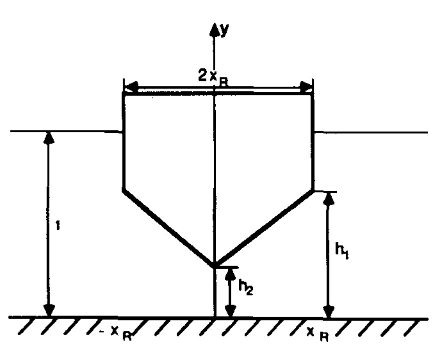

Figure 4. Case 2: $h_1 = 0{\cdot}7$, $h_2 = 0{\cdot}3$, $x_R = 0{\cdot}5$. Case 3: $h_1 = 0{\cdot}7$, $h_2 = 0{\cdot}7$, $x_R = 0{\cdot}5$. Case 4: $h_1 = 0{\cdot}7$, $h_2 = 0{\cdot}3$, $x_R = 2$

time when η^+_{max} occurs; η^-_{max}, the maximum surface wave elevation at $\zeta=\zeta_L$; t^-_{max}, the time when η^-_{max} occurs; H_T, the amplitude of the transmitted solitary wave. The fluid masses in the fields $\Sigma_1+\Sigma_2$ and $\Sigma_4+\Sigma_5$ as well as the total fluid mass in the whole field are defined respectively as

$$m_L(s\Delta t)=\Delta x\sum_{i=0}^{M}\eta_L(-i\Delta x-x_L, s\Delta t),$$

$$m_R(s\Delta t)=\Delta x\sum_{i=0}^{M}\eta_R(i\Delta x+x_R, s\Delta t),$$

$$m(s\Delta t)=m_R(s\Delta t)+m_L(s\Delta t),$$

where η_L and η_R are given by equations (63) and (64). The maximum relative error of the fluid mass is defined by

$$E_r=\frac{\max|m(s\Delta t)-m_0|}{m_0}\,\%,\qquad 0\leqslant s\leqslant N.$$

Here m_0 is the the initial mass of the flow field and N is the prescribed total number of time steps; in this paper $N=300$.

The time histories of the wave elevations in the fields $\Sigma_4+\Sigma_5$ and $\Sigma_1+\Sigma_2$ for case 1 are plotted respectively in Figures 5 and 6. In fact they are also the typical trends of the wave behaviour around the structure for all the situations considered. It is observed that like the incident wave, the transmitted wave is also a solitary wave (see Figure 6), while the reflected wave is a permanent form wave with the trough (see Figure 5).

Some computed characteristic quantities for cases 1–4 and the variation of m_L, m_R and m with time in case 1 are listed respectively in Tables I and II.

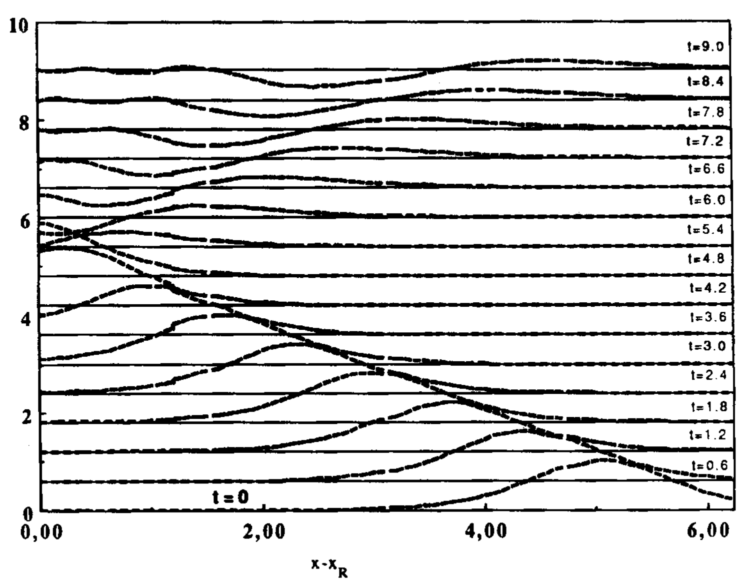

Figure 5. Time history of the wave elevation in $\Sigma_4+\Sigma_5$

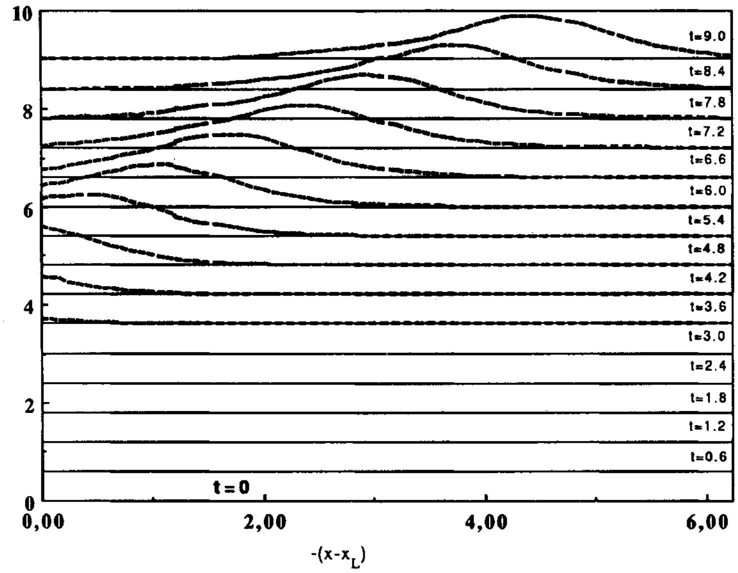

Figure 6. Time history of the wave elevation in $\Sigma_1+\Sigma_2$

Table I. Computed characteristic parameters in cases 1–4

Case	η^+_{max}	t^+_{max}	η^-_{max}	t^-_{max}	H_T	E_r
1	1·390	4·530	0·775	5·010	0·836	3·418
2	1·351	4·530	0·859	4·980	0·876	2·828
3	1·262	4·530	0·926	4·860	0·902	1·983
4	1·600	4·560	0·464	5·250	0·576	5·421

Table II. Variation of m_L, m_R and m with time in case 1

t	m	m_L	m_R
0·0	1·6330	1·6330	0·0000
0·6	1·6330	1·6330	0·0000
1·2	1·6330	1·6329	0·0001
1·8	1·6330	1·6325	0·0005
2·4	1·6329	1·6305	0·0025
3·0	1·6327	1·6207	0·0120
3·6	1·6309	1·5761	0·0548
4·2	1·6162	1·3972	0·2190
4·8	1·5772	0·9548	0·6224
5·4	1·5914	0·4712	1·1201
6·0	1·6211	0·1758	1·4453
6·6	1·6269	0·0430	1·5839
7·2	1·6283	−0·0013	1·6296
7·8	1·6278	−0·0127	1·6405
8·4	1·6282	−0·0147	1·6429
9·0	1·6279	−0·0153	1·6432

Table III. Effect of number of boundary elements on the computation

Result*	η_{max}^{+}	t_{max}^{+}	η_{max}^{-}	t_{max}^{-}	H_T	E_r
1	1·390	4·530	0·775	5·010	0·836	3·418
2	1·400	4·530	0·771	4·996	0·839	3·420

* For result 1, $n_L = n_R = 30$, $n_s = 60$ and $n_b = 30$; for result 2, $n_L = n_R = 15$, $n_s = 50$ and $n_b = 16$.

From Table I one can see that for the cases shown in Figure 4 the change in h_2 has a significant effect on the wave behaviour and the influence of the structure horizontal dimension is determinant. A decrease in h_2 results in increases of t_{max}^{-} and η_{max}^{+}. Since the area of Σ_3 in case 1 is smaller than that in case 2, more time is needed for the same quantity of fluid to go through Σ_3. Therefore the interaction of the structure and the waves is relatively stronger. Consequently, t_{max}^{-} and η_{max}^{+} increase and η_{max}^{-} decreases. In case 4, for which the computation was performed using $n_L = n_R = 20$, $n_s = 100$ and $n_b = 80$, the structure horizontal dimension is four times that of cases 1–3. As a result, the value of the amplitude of the transmitted solitary wave, 0·575, is comparable to the values of the crest and the trough of the reflected wave, 0·47 and 0·37 respectively. In addition, in all the sample computations the values of E_r are of the order of the approximation adopted, i.e. $O(\alpha\beta^{1/2}) = 0{\cdot}06$ (see Table I), which indicates that the numerical algorithm used here conserves the expected order of approximation. Table II shows that larger differences between m and m_0 occur from $t = 4{\cdot}2$ to $t = 5{\cdot}4$ when the error introduced is due to the approximation for (27), and the total fluid mass recovers gradually to its initial mass m_0, i.e. the present method describes correctly the conservation of mass for shallow water waves in the far field.

Numerical experiments were also conducted with different numbers of boundary elements in order to determine how many boundary elements are required for an acceptable solution to be obtained. For case 1 a comparison of the results obtained using two different sets of boundary elements is given in Table III.

In all these sample computations it is found that 20 boundary elements are sufficient for the discretization of the boundaries $\zeta = \zeta_L$ and $\zeta = \zeta_R$ and that the number of elements over $y = b(\zeta)$ and $y = 0$ should be adapted to changes of the structure horizontal dimension. Also, if keeping the maximum boundary element length smaller than 0·06, then the maximum relative difference, i.e. the ratio of the difference between two quantities and either of the two quantities, of the characteristic parameters computed using different sets of boundary elements remains smaller than 0·02 (e.g. see Table III).

5. CONCLUSIONS

A numerical method has been developed for computation of the non-linear shallow water waves diffracted by a structure of arbitrary bottom shape. The method involves application of the matched asymptotic expansion, the boundary element method and the finite difference approximation, and a time-stepping procedure is used to obtain the evolution of the waves.

ACKNOWLEDGEMENT

The author is particularly grateful to a referee for his very helpful and illuminating comments which have led to the improvements in the work.

REFERENCES

1. M. Isaacson, 'Nonlinear wave effect on the fixed and floating bodies', *J. Fluid Mech.*, **120**, 267–281 (1982).
2. N. Sugimoto and T. Kakutani, 'Reflection of a shallow-water soliton, Part 1. Edger layer for shallow-water waves', *J. Fluid Mech.*, **146**, 369–382 (1984).
3. Q. Q. Lu, Y. Z. Liu, G. P. Miao and D. X. Zhu, 'Transmission and reflection of a planar soliton', *Adv. Hydrodyn.*, **4**, 68–78 (1987).
4. Q. Q. Lu and Y. Z. Liu, 'Reflection of a solitary wave at the coastline with a slot', *Acta Mech. Sinica*, **21**, 161–167 (1989).
5. C. C. Mei, *Applied Dynamics of Ocean Surface Waves*, Wiley, New York, 1983.
6. R. W. Yeung, 'Numerical methods in free-surface flows', *Ann. Fluid Mech.*, **14**, 395–442 (1982).
7. C. A. Brebbia, *The Boundary Element Method for Engineers*, Pentech, London, 1978.
8. Q. Q. Lu, 'The soliton generated by a moving boundary', *Chinese J. Comput. Phys.*, **6**, 51–57 (1989).
9. Q. Q. Lu, 'The soliton solution of the initial-boundary value problem of the Boussinesq equations', *Chinese J. Comput. Phys.*, **7**, 11–16 (1990).
10. H. Power and A. T. Chwang, 'On the reflection of a planar solitary wave at a vertical wall', *Wave Motion*, **6**, 183–195 (1984).